

# Fail-Operational Shock Detection and Correction of MEMS-based Micro-Scanning LiDAR Systems

Philipp Stelzer\*, Andreas Strasser\*, Christian Steger\*, and Norbert Druml†

\*Graz University of Technology, Graz, Austria

{stelzer, strasser, steger}@tugraz.at

†Infineon Technologies Austria AG, Graz, Austria

{norbert.druml}@infineon.com

**Abstract**—Highly automated or autonomous vehicles will be dependent on systems that have to perceive the environment to make valid decisions during the driving cycle. One of the key enablers for autonomous and highly automated vehicles will be Light Detection And Ranging (LiDAR) technology. A Micro-Electro-Mechanical System (MEMS) based Micro-Scanning LiDAR is able to detect obstacles in a predefined Field-of-View (FoV). The point cloud stability of the scanned FoV is mandatory to be able to make a valid point where the obstacle is located in the scenery. Due to the fact that massive shocks can occur arbitrarily to the system, it is necessary to be able to detect and correct them as fast as possible that point cloud stability can be recovered as fast as possible. In this paper, we introduce a novel system architecture that enables a fast shock detection and correction of phase and frequency for MEMS-based Micro-Scanning LiDAR Systems. Our novel introduced fail-operational detection and correction system architecture was implemented in a 1D MEMS-based Micro-Scanning LiDAR FPGA platform to prove its feasibility and for performance evaluation.

**Index Terms**—LiDAR, 1D MEMS Mirror, automated driving, fast shock correction, failure recovery system

## I. INTRODUCTION

Safety is a really sensitive topic in automotive applications, at least since Advanced Driver-Assistance Systems (ADAS) are integrated into vehicles. If the safety of such ADAS is not ensured, automated driving cannot be possible in any case. [2] There are so-called SAE levels, which indicate the degree of automation of the vehicle. [3] The SAE Level is declared by reference to the integrated systems in a vehicle, which are responsible for enabling automated driving. Currently, fault-tolerant systems are applying the fail-safe approach. Fail-safe

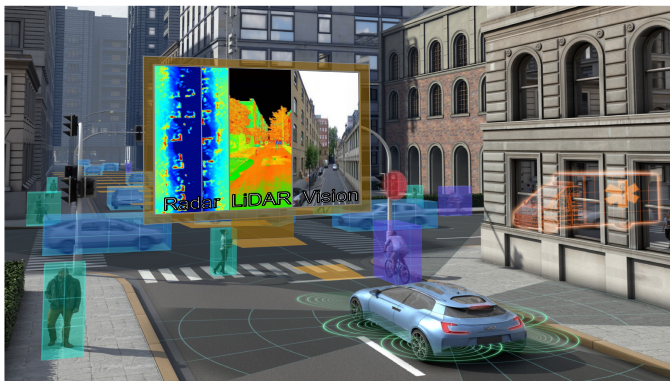


Fig. 1. PRYSTINE's concept view of a Fail-operational Urban Surround perceptiON (FUSION). [1]

means that the system either directly possesses a safe state or is brought to a safe state by a special action if a failure occurs; it can also be a system shutdown. Due to highly automated vehicles in the future, it is mandatory that systems which are responsible for driving operation have to be fault-tolerant. Regarding this, systems of future highly automated vehicles have to be fail-operational. A fail-operational system tolerated at least one failure and stays operational at least degraded. [4] How the State-of-the-Art (SoA) architecture of such systems has to be built up is described by Temple et al. [5] Due to the reason that we are considering our system as a sensor of the overall system architecture, we pursued a different approach for developing a fail-operational architecture for a MEMS-based LiDAR sensor system. Nevertheless, a LiDAR-based sensor system will not be sufficient for an environment perception by a highly automated vehicle. Therefore, the PRogrammable sYSTEMs for INtelligence in automobiles (PRYSTINE) project is aiming a Fail-operational Urban Surround perceptiON (FUSION). [1] The FUSION of PRYSTINE is based on robust RADAR and LiDAR sensor fusion and control functions, illustrated in Figure 1, in order to enable safe automated driving in urban and rural environments. Thus, it is necessary to ensure also failure safety in the sensors, which are embedded in the overall environment perception system. Hence, this paper is dealing with a fail-operational architecture for a MEMS-based LiDAR system. The remainder of the paper is structured as follows. Background information about safety states will be provided in section II. The overview of related work on MEMS-based LiDAR systems is given in section III. The novel architecture with higher robustness against external problems will be introduced in detail in section IV, and the achieved results, including a short discussion, will be provided in section V. A summary and short discussion of the findings will conclude this paper in section VI.

## II. BACKGROUND

In safety-related systems, especially in automotive applications for highly automated driving, it has to be ensured that obtained sensor data is correct or at least corrupted data is detectable, and the system can make arrangements accordingly. Kohn et al. [6] are describing two kinds of approaches that are common to avoid or minimize a system failure. In Figure 2 is depicted, how they want to achieve this risk minimization.

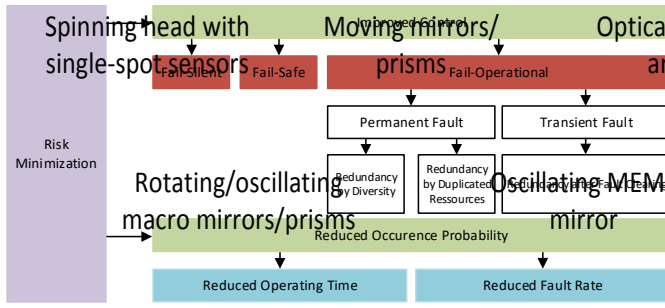


Fig. 2. Realization of risk minimization. [6]

The only optional approach for a safety-relevant automotive application is to minimize the risk either by implementing an improved control, like a safe shutdown or a higher fault tolerance. [6] We regard our LiDAR sensor system only as a part of the entire environment perception system and hence pursue another approach.

#### A. Fail-Silent

The system stays passive and does not influence other components or systems in a wrong way. [4]

#### B. Fail-Safe

If there are detected non-tolerable failures, the system switches to a safe system state. The system distinguishes two possible states, either the application is executed unaffected, or the system is stopped. [4, 6]

#### C. Fail-Operational

The occurrence of a failure is tolerated; the system stays operational. [4] To achieve fail-operational behaviour, SoA solutions must be designed redundantly and/or diversely. [6] In our paper, a novel approach is used to achieve a fail-operational behaviour for the LiDAR sensor system.

### III. RELATED WORK

Until recently, only bulky LiDAR systems like the Velodyne HDL-64E LiDAR were available on the market. [8] Therefore, industry and academia are encouraged to research low-cost, robust, and automotive qualified LiDARs. The answer can be the MEMS technology. MEMS mirrors are already used for optical scanners. [9–11] However, the problem of strong shocks and their consequences on the MEMS mirrors were neglected so far, since most applications are stationary. [11] But in recent years there was the MEMS mirror technology also introduced into the automotive domain. [7, 12–14] Druml et al. [7, 14] have introduced a MEMS-based LiDAR system.

#### A. 1D MEMS Micro-Scanning LiDAR

Here, the 1D MEMS Micro-Scanning LiDAR concept by Druml et al. is introduced. In Figure 3, the entire system architecture of Druml et al.’s LiDAR system is illustrated. An oscillating 1D MEMS mirror, a MEMS Driver ASIC, a laser illumination unit, a System Safety Controller (AURIX) [15], a Receiver Circuit and an array of photo diodes form the entire chipset. The MEMS Driver ASIC is responsible for accurately

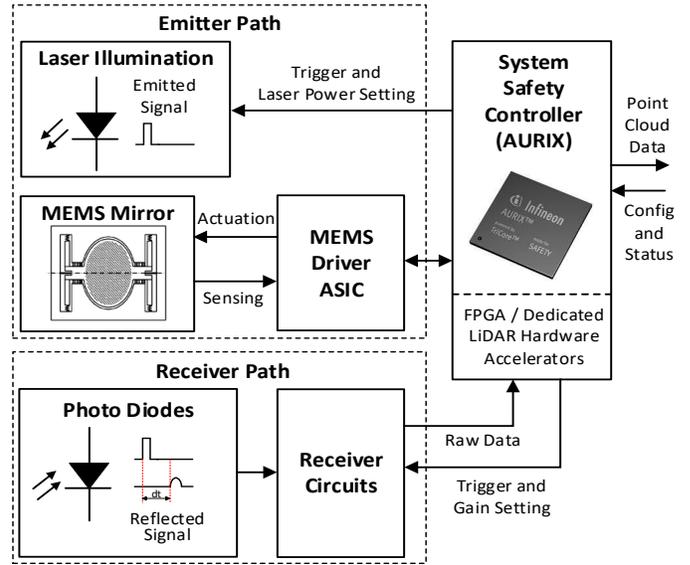


Fig. 3. System concept of a 1D MEMS-based automotive LiDAR system by Druml et al. [7]

operating the MEMS mirror. To achieve correct operation of the MEMS mirror, the MEMS Driver ASIC besides actuating the MEMS mirror is also sensing and controlling its movement. [7] How an illumination of a scenery works by a 1D micro-scanning LiDAR is depicted in Figure 4. By this idea, laser beams are shot onto the 1D MEMS mirror and form a vertical line. Due to the oscillation of the MEMS mirror, this vertical line is moved horizontally across the Field-of-View (FoV). In the FoV located obstacles reflected the light and a stationary detector captures it. [7]

One of the most critical components of the MEMS-based LiDAR system is the MEMS Driver. It is providing crucial signals to the System Safety Controller (AURIX). These signals are relevant to be able to monitor the current status of the mirror during operation. Thus, there are essential tracking signals, depicted in Figure 5, like the POSITION\_L (signal on logical high represents a MEMS mirror alignment to the left; else on the right) and the DIRECTION\_L (signal on logical high represents a movement to the left; else on the right) which provide accurate information about the MEMS mirror’s position. [7]

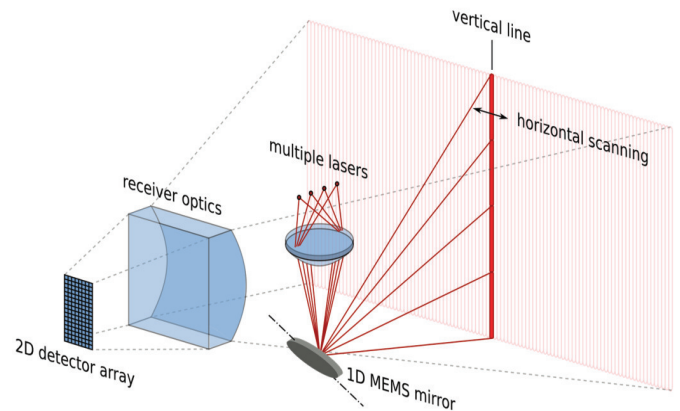


Fig. 4. 1D micro-scanning LiDAR functional principle. [7]

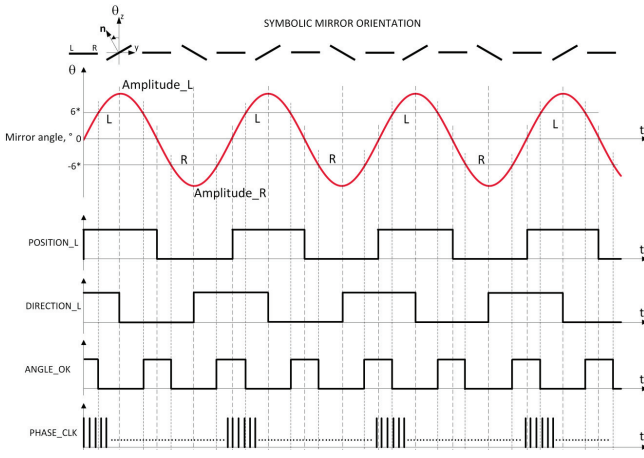


Fig. 5. Essential MEMS mirror signals of the MEMS Driver ASIC. [7]

The maximum deflection angle of the MEMS mirror derives from the actuation frequency and High Voltage (HV). There are two options to operate the MEMS mirror, either the open-loop or closed-loop operation. [16] For regular operation is a closed-loop control strategy used. The mechanical behaviour of the MEMS mirror is described, as seen in Figure 6, as a non-linear harmonic oscillator. In the beginning, the MEMS mirror's operation point is located on the lower resonance curve. Thus, the start frequency has to be decreased until the operation point has been reached the jump frequency  $f_{jump}$ . At  $f_{jump}$ , the MEMS mirror jumps onto the upper resonance curve. That can be observed by a recognizable change in phase relation and the mirror's maximum deviation angle. After the mirror reaches the upper resonance curve, the PLL mode will be activated. Due to given physical limits, the MEMS mirror is able to be operated on the upper resonance curve between  $f_{jump}$  and the fall-back frequency  $f_{fb}$ .

### B. Problem-Situation with Common PLL

Principally, the PLL is responsible for correcting a mismatch in phase and frequency between the Driver and MEMS mirror due to the lock on the phase of the reference signal. [17] But under certain circumstances, like distorted utility conditions during operation of a PLL [18], it is possible that an out of

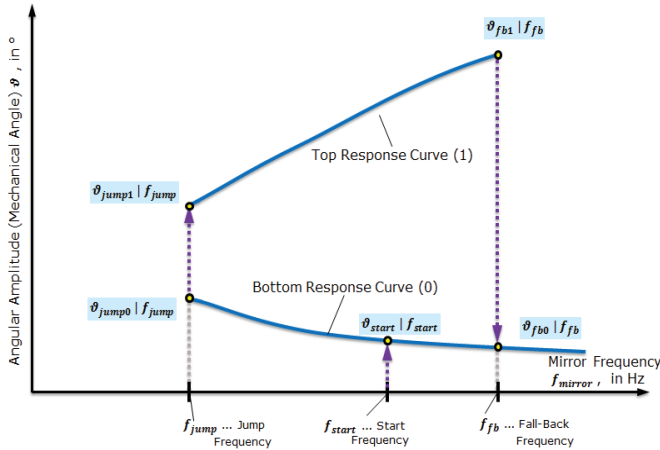


Fig. 6. Druml et al.'s MEMS mirror response curve. [7]

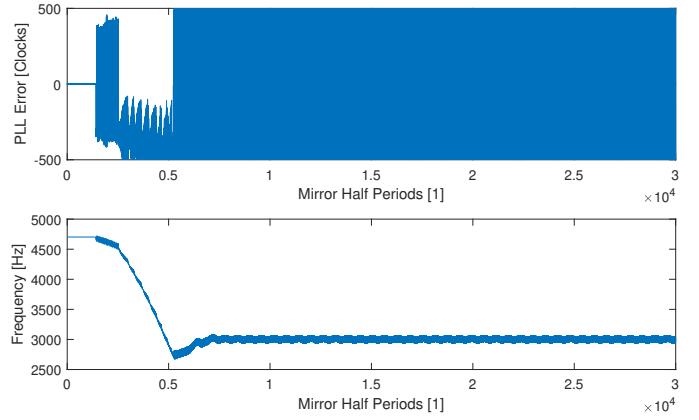


Fig. 7. Measurement of the effects of PLL lock loss after a fatal shock was injected into the LiDAR system.

lock can appear in PLLs. [19, 20] It is already known that vibrations can cause positioning errors in airborne LiDAR systems. Ma et al. [21] showed it by reference to their analysis. Furthermore, in the automotive sector, vibration stresses on mechanical components such as mechanical connectors are already taken into account in standards like "USCAR-2". [22] Consequently, it is to be expected that vibrations will also have an effect on automotive LiDAR systems. If vibrations affect automotive LiDAR systems, also unintended shocks will do it. Therefore, it is assumed that unexpected shocks will affect the MEMS mirror's movement.

Thus, in Figure 7 it is illustrated a simulation of fatal shock affecting the 1D MEMS-based LiDAR System. It is clearly seen that fatal shocks can cause a loss of phase and frequency in a controlled system with a SoA PLL. Strasser et al. [23] solved it with a fast system restart, which could take too long, however, for a safety-critical state.

This gives rise to the following research questions, which are dealt with in this article:

- Is it possible to correct phase and frequency of a MEMS-based LiDAR System after it is seriously shocked during runtime?
- If it is possible to correct phase and frequency during runtime, is it possible to do so in an acceptable time?

## IV. FAIL-OPERATIONAL SHOCK DETECTION AND CORRECTION OF MEMS-BASED LIDAR SYSTEMS

In this section, we introduce our adapted architecture to introduce fail-operational behaviour into our MEMS-based LiDAR System. In Figure 8 is in black a simplified, common used PLL depicted. The red additions complete the architecture of the novel introduced architecture with fail-operational behaviour. Supplementary blocks are the Phase Frequency Detection and Correction (PFDC) unit, the Shock Detection (SD) subunit in the Phase Detector (PD) block, and the Shock HV(ON/Off) (SHV) subunit in the Mirror Subtiming block. Essential signals for the functionality of the phase frequency detection and correction are Correction Enable (CorrEn), Digitally Controlled Oscillator Correction (DCOcorr), Phase Counter Correction (PCcorr), Switch Enable

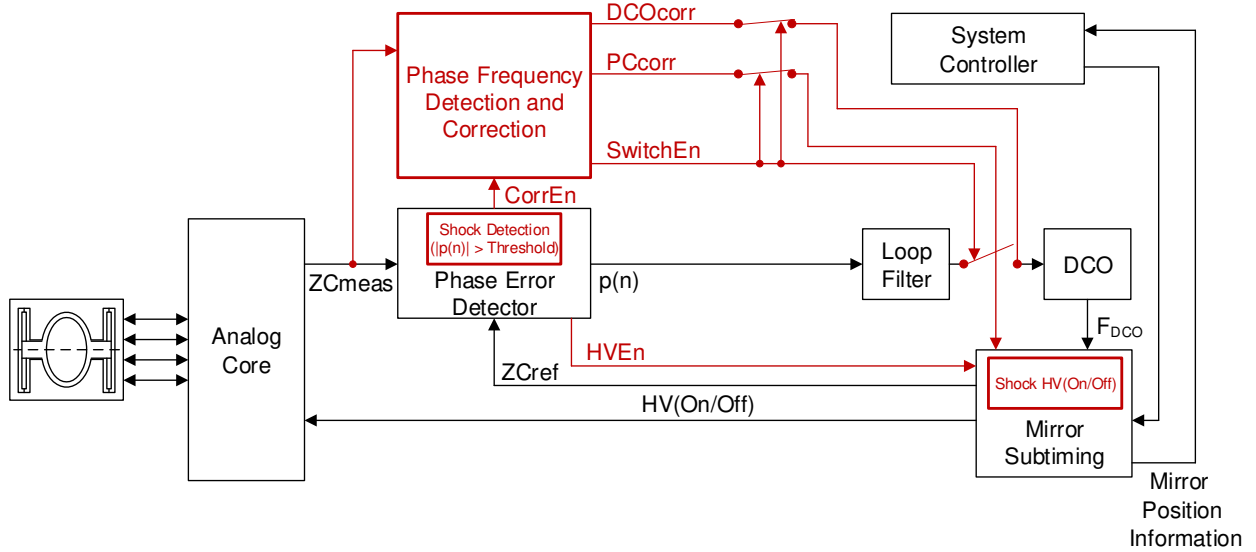


Fig. 8. Block diagram of a PLL architecture with the novel adaptations to include a fail-operational behaviour in the system.

(SwitchEn) and High Voltage Enable (HVEN). The description of the blocks and signals follows in the succeeding subsection, in which the procedure is elucidated. After the subsection with the procedure, an additional subsection of the test procedure is introduced. There the used hardware and the way in which the shocks of the MEMS mirror were simulated are specified.

#### A. Process Flow of the Novel Procedure

The process flow, after a threshold value of the phase error, is exceeded, is illustrated in Figure 9. The phase frequency correction is divided into the following states:

##### 1) INIT State

In the beginning, the PFDC unit is disabled, and all values for phase and frequency detection are reset. The most essential value is the Zero Crossing Timing Counter (ZCTC), which is later mandatory for frequency determination. As long as the PLL error is lower than the predefined threshold, the PLL is responsible for phase and frequency synchronization between the MEMS mirror and MEMS Driver.

##### a) Threshold Value Exceedance

After the threshold is exceeded, the CorrEn signal enables the novel Phase-Frequency-Detector (PFD) in the PFDC block.

##### b) No Threshold Value Exceedance

As long as the predefined threshold is not exceeded, the PFDC unit remains switched off. The HV is switched on and off at predefined points of time in the Mirror Subtiming block.

##### 2) State 1

To be able to detect a Zero Crossing (ZC), it is mandatory that the HV is on. Hence, it will be permanently turned on by the HVEN signal. As long as no ZC occurs, the condition is maintained. After a ZC is detected, the state is switched to State 2.

##### 3) State 2

With the first detected ZC, the ZCTC will be enabled to count up. With every rising clock, the value is increased.

This happens until the next ZC occurs. With the second ZC, the ZCTC stops with counting, and the state is changed to state 3.

##### 4) State 3

The ZCTC will be used for calculating the frequency.

$$DCO_{corr} = \frac{DCO_{max} \cdot \text{Subtiming range}}{ZCTC} \quad (1)$$

In Equation 1, the corrected DCO increment will be calculated by reference to the maximum possible DCO

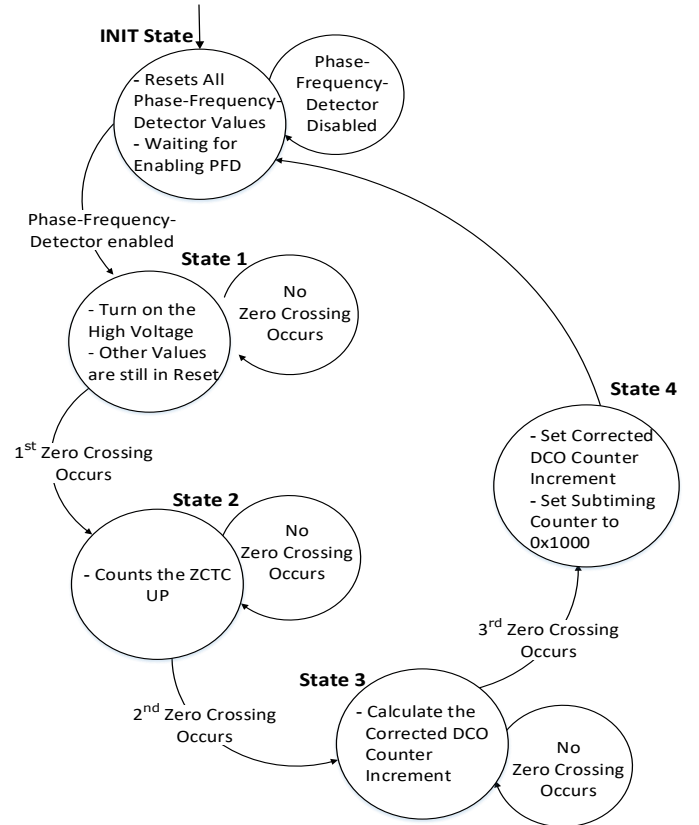


Fig. 9. Process flow of the Phase Frequency Detection and Correction module.



in contrast to 11 m and at 130 km/h after 25 cm in contrast to 18 m. For highly automated applications, a fail-operational behaviour of environment perception systems will be mandatory. Thus, the novel detection and correction procedure will be a key enabler for fail-operational environment perception. The overall objective hence is to ensure a safe driving state for passengers and other road participants now and in the future.

#### ACKNOWLEDGMENTS

The authors would like to thank all national funding authorities and the ECSEL Joint Undertaking, which funded the PRYSTINE project under the grant agreement number 783190.

PRYSTINE is funded by the Austrian Federal Ministry of Transport, Innovation and Technology (BMVIT) under the program ICT of the Future between May 2018 and April 2021 (grant number 865310). More information: <http://iktderzukunft.at/en/>.

#### REFERENCES

- [1] N. Druml, G. Macher, M. Stolz, E. Armengaud, D. Watzenig, C. Steger, T. Herndl, A. Eckel, A. Ryabokon, A. Hoess, S. Kumar, G. Dimitrakopoulos, and H. Roedig, "PRYSTINE - PRogrammable sYSTEMs for INtelligence in Automobiles," in *2018 21st Euromicro Conference on Digital System Design (DSD)*, Aug 2018, pp. 618–626.
- [2] A. Kohn, R. Schneider, A. Vilela, A. Roger, and U. Dannebaum, "Architectural Concepts for Fail-Operational Automotive Systems," in *SAE 2016 World Congress and Exhibition*. SAE International, April 2016.
- [3] SAE, "SAE International Standard J3016 - Taxonomy and Definitions for Terms Related to On-Road Motor Vehicle Automated Driving Systems," SAE International, Standard, January 2014.
- [4] R. Isermann, "Mechatronic systems—Innovative products with embedded control," *Control Engineering Practice*, vol. 16, no. 1, pp. 14 – 29, 2008.
- [5] C. Temple and A. Vilela, "Fehlertolerante Systeme im Fahrzeug – von "Fail-Safe" zu "Fail-Operational"," in *Elektroniknet*, July 2014.
- [6] A. Kohn, M. Kmeyer, R. Schneider, A. Roger, C. Stellwag, and A. Herkersdorf, "Fail-Operational in Safety-Related Automotive Multi-Core Systems," in *10th IEEE International Symposium on Industrial Embedded Systems (SIES)*, June 2015, pp. 1–4.
- [7] N. Druml, I. Maksymova, T. Thurner, D. Van Lierop, M. Hennecke, and A. Foroutan, "1D MEMS Micro-Scanning LiDAR," in *The Ninth International Conference on Sensor Device Technologies and Applications (SENSORDEVICES 2018)*, 09 2018.
- [8] Velodyne LiDAR, "HDL-64E," 2016.
- [9] B. Yang, L. Zhou, X. Zhang, S. Koppal, and H. Xie, "A compact MEMS-based wide-angle optical scanner," in *2017 International Conference on Optical MEMS and Nanophotonics (OMN)*, Aug 2017, pp. 1–2.
- [10] X. Zhang, L. Zhou, , , S. Koppal, Q. Tanguy, and H. Xie, "A wide-angle immersed MEMS mirror and its application in optical coherence tomography," in *2016 International Conference on Optical MEMS and Nanophotonics (OMN)*, July 2016, pp. 1–2.
- [11] W. M. Zhu, W. Zhang, H. Cai, J. Tamil, B. Liu, T. Bourouina, and A. Q. Liu, "A MEMS digital mirror for tunable laser wavelength selection," in *TRANSDUCERS 2009 - 2009 International Solid-State Sensors, Actuators and Microsystems Conference*, June 2009, pp. 2206–2209.
- [12] L. Ye, G. Zhang, Z. You, and C. Zhang, "A 2D resonant MEMS scanner with an ultra-compact wedge-like multiplied angle amplification for miniature LIDAR application," in *2016 IEEE SENSORS*, Oct 2016, pp. 1–3.
- [13] U. Hofmann, F. Senger, F. Soerensen, V. Stenchly, B. Jensen, and J. Janes, "Biaxial resonant 7mm-MEMS mirror for automotive LIDAR application," in *2012 International Conference on Optical MEMS and Nanophotonics*, Aug 2012, pp. 150–151.
- [14] H. W. Yoo, N. Druml, D. Brunner, C. Schwarzl, T. Thurner, M. Hennecke, and G. Schitter, "MEMS-based lidar for autonomous driving," *e & i Elektrotechnik und Informationstechnik*, vol. 135, no. 6, pp. 408–415, Oct 2018.
- [15] Infineon Technologies AG. (2018) AURIX System Safety Controller. <https://iot-automotive.news/aurix-microcontroller-tc3xx-family-infineon-fuels-automated-driving-electromobility>.
- [16] B. Borovic, A. Q. Liu, D. Popa, H. Cai, and F. L. Lewis, "Open-loop versus closed-loop control of MEMS devices: choices and issues," *Journal of Micromechanics and Microengineering*, vol. 15, no. 10, p. 1917, 2005.
- [17] G.-C. Hsieh and J. C. Hung, "Phase-locked loop techniques. A survey," *IEEE Transactions on industrial electronics*, vol. 43, no. 6, pp. 609–615, 1996.
- [18] V. Kaura and V. Blasko, "Operation of a phase locked loop system under distorted utility conditions," *IEEE Transactions on Industry Applications*, vol. 33, no. 1, pp. 58–63, Jan 1997.
- [19] T. Endo and L. O. Chua, "Chaos from phase-locked loops," *IEEE Transactions on Circuits and Systems*, vol. 35, no. 8, pp. 987–1003, 1988.
- [20] P. Wang, "Chaos In Phase Locked Loop," in *2006 International Symposium on VLSI Design, Automation and Test*, April 2006, pp. 1–2.
- [21] H. Ma and J. Wu, "Analysis of positioning errors caused by platform vibration of airborne LiDAR system," in *2012 8th IEEE International Symposium on Instrumentation and Control Technology (ISICT) Proceedings*, July 2012, pp. 257–261.
- [22] SAE, "Performance Specification for Automotive Electrical Connector Systems USCAR2-4," SAE International, Standard, May 2004.
- [23] A. Strasser, P. Stelzer, C. Steger, and N. Druml, "Speed-Up of MEMS Mirror's Transient Start-Up Procedure," March 2019, 2019 IEEE Sensors Applications Symposium, SAS ; Conference date: 11-03-2019 Through 13-03-2019.